

Earth and Planetary Science Letters 176 (2000) 443-455

EPSL

www.elsevier.com/locate/epsl

Rock-magnetic carriers of century-scale susceptibility cycles in glacial—marine sediments from the Palmer Deep, Antarctic Peninsula

Stefanie A. Brachfeld*, Subir K. Banerjee

Department of Geology and Geophysics, Institute for Rock Magnetism, University of Minnesota, Minneapolis, MN 55455, USA

Received 26 August 1999; received in revised form 10 January 2000; accepted 11 January 2000

Abstract

A 4200 year long magnetic susceptibility profile from the Palmer Deep records century- and millennial-scale variability in paleoenvironmental conditions along the western Antarctic Peninsula. The susceptibility profile shows regularly spaced highs and lows over the last 3360 years B.P. then drops to uniformly low values. These features are formed by the variable dilution of terrigenous material with biogenic sediments and shifts in magnetic mineralogy. High-susceptibility intervals are characterized by multi-domain (MD) pure magnetite. Low-susceptibility intervals are characterized by pseudo-single-domain (PSD) magnetite and titanomagnetite. Prior to 3360 years B.P., the magnetic mineral assemblage is dominated by fine PSD titanium-rich titanomagnetite and superparamagnetic particles, suggesting a change in sediment provenance and/or sediment transport processes. The absence of MD magnetite suggests a cessation in locally derived ice-rated debris. This horizon represents the transition from the mid-Holocene climatic optimum to the Neoglacial period, marked by an increase in glacial sedimentation. © 2000 Published by Elsevier Science B.V. All rights reserved.

Keywords: magnetic susceptibility; magnetic minerals; paleoclimatology; Antarctic Peninsula

1. Introduction

During historical times, the Antarctic Peninsula has experienced a warming trend, a reduction in the extent of ice shelves, and a redistribution of penguin species (e.g. [1]). The cause of these

changes is presently unknown, but may involve both natural and anthropogenic components. Coring operations and sediment trap studies were initiated approximately 10 years ago in order to gain a better understanding of the regional glacial and biogenic sedimentation processes and to investigate the natural environmental variability over time (e.g. [1–3]).

Biosiliceous sediment cores recovered from the Palmer Deep, the Gerlache Strait and Andvord Bay (Fig. 1) that span the last ~ 4000 years show a remarkably similar magnetic susceptibility profile. Over the past ~ 3500 years, these records

Fax: +1-612-625-7502; E-mail: brach002@tc.umn.edu

0012-821X/00/\$ - see front matter © 2000 Published by Elsevier Science B.V. All rights reserved.

PII: S0012-821X(00)00008-X

^{*} Corresponding author. 108 Pillsbury Hall, 310 Pillsbury Drive, Minneapolis, MN 554455, USA.

show regularly spaced peaks and troughs in magnetic susceptibility that are caused, in part, by pulses in biogenic sedimentation that have been interpreted as periodic diatom blooms [4–6]. Prior to 3500 years B.P., magnetic susceptibility was uniformly low. Spectral analysis of these records has revealed strong periodicities at 400, ~200 and 50–70 years [6,7]. The striking similarity of the susceptibility records from sites along the Peninsula has led to an interest in correlating individual susceptibility features both regionally and farther afield with century-scale events in late Holocene records (e.g. [4,8]). Further, magnetic susceptibility has been proposed as a proxy indicator of paleoproductivity for this region [5].

Correlation based on magnetic susceptibility records and development of magnetic susceptibility as an environmental proxy requires an understanding of the magnetic mineral assemblage that carries the signal and the local sedimentation processes that generate the assemblage. Therefore, we have undertaken a detailed study of glacial—marine sediments from the Palmer Deep, a basin on the western margin of the Antarctic Peninsula. Our purpose here is to characterize the magnetic mineral assemblage that records the century-scale susceptibility features, and to explain the assemblage in terms of glacial, biogenic and chemical sedimentation processes.

2. Geologic setting

The Palmer Deep is a bathymetric depression located 20 km south of Anvers Island (Fig. 1). Seismic and bathymetric surveys were carried out on several occasions, during cruise 92-02 of the R.V. *Polar Duke* (U.S. Antarctic Program), during the February 1997 cruise of the R.V. *OGS-Explora* (Programma Nazionale Ricerche in Antartide) and during cruise 99-03 of the R.V. *Nathaniel B. Palmer* (U.S. Antarctic Program) [5,9]. The basin has a complex geometry, with a large depocenter bounded by the 1000 m contour. This study focuses on core PD92-30 (64°51.720′S, 64°12.506′W) which was collected during cruise 92-02 of the R.V. *Polar Duke* in a water depth of 1040 m.

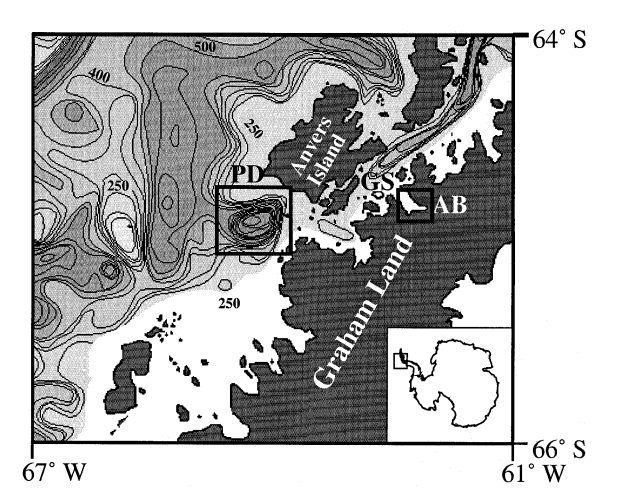


Fig. 1. Location of the Palmer Deep (PD), Andvord Bay (AB) and the Gerlache Strait (GS). The bathymetry contour interval is 50 m. The bathymetry data are from [25].

3. Chronology

Radiocarbon dating of material from several cores collected by the United States Antarctic Program and during Ocean Drilling Program (ODP) Leg 178 contributed to the Palmer Deep chronology. Dates were obtained from bulk organic carbon, foraminiferal calcite and mollusk shells. A detailed discussion of the dated material, derivation of a reservoir correction, and a synthesis of 36 radiocarbon dates from the Palmer Deep are presented by Domack et al. (submitted) [7]. This new age model places the base of PD92-30 at approximately 4200 years B.P.

4. Experimental methods

Volume-normalized whole-core magnetic susceptibility (hereafter referred to simply as susceptibility) of PD92-30 was measured at 5 cm intervals with a Bartington MS2B at the Antarctic Research Facility at Florida State University. Subsamples of 100–200 mg were collected at 20–50 cm intervals. Large intervals occur where the core has already been heavily sampled. Samples were freeze-dried for magnetic granulometry analyses performed at the Institute for Rock Magnetism at the University of Minnesota. Room tem-

perature and low-temperature (20–300 K) measurements were made on bulk sediment samples. High-temperature measurements were made on magnetic material extracted from the sediment. The extracts were obtained by continuously recirculating a sediment slurry past a rare earth magnet for a minimum of 7 days. We measured concentration-dependent parameters (ferromagnetic susceptibility, saturation magnetization and saturation remanence) of the bulk sediment and residual sediment slurries to monitor the efficiency of the extraction process. The above parameters were reduced by factors of 5–52 in the residual slurries [10].

Low-field mass-normalized susceptibility (χ_{LF}) was measured using a Geofyzika KLY-2 Kappabridge. Hysteresis parameters, high-field mass-normalized susceptibility (χ_{HF}) and Curie temperatures were measured on a Princeton Measurements Corp. MicroMag Vibrating Sample Magnetometer. Curie temperatures were determined

from the temperature dependence (0-700°C) of the saturation magnetization (M_S) of a sample in a 1 T field. Measurements were made in a helium gas atmosphere in order to minimize alteration of the sample during heating. Low-temperature remanence and susceptibility measurements were made from 20 to 300 K using a Quantum Design MPMS2 SQUID magnetometer. At each temperature step from 20 to 300 K, the susceptibility was measured at frequencies of 10, 31, 99, 310 and 997 Hz. X-ray diffraction (XRD) spectra were determined from magnetic extracts using a Philips XRG 3100 X-ray powder diffractometer. Energy-dispersive X-ray spectra (EDS) were determined from magnetic extracts using a JEOL 8900 Electron Probe Microanalyzer.

5. Stratigraphy and physical properties

PD92-30 consists of olive green to dark olive

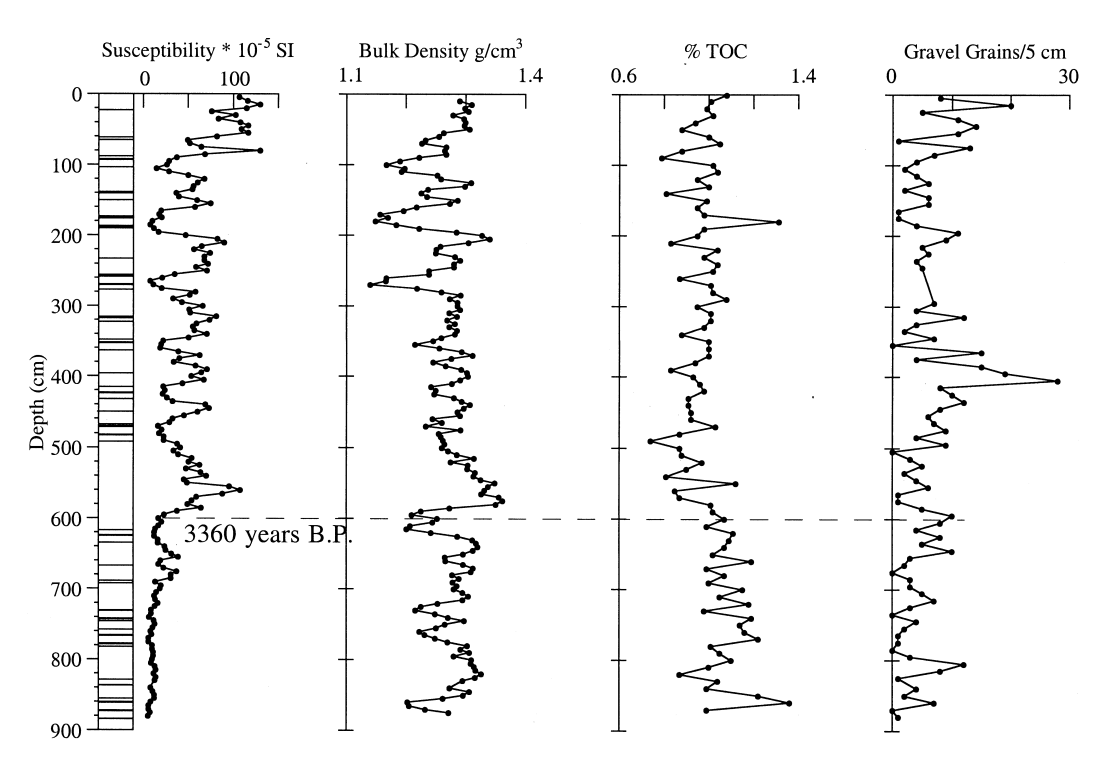


Fig. 2. Sediment texture and physical properties of PD92-30 [6]. Solid intervals in the stratigraphic column denote massive sediment texture. Horizontal lines denote thinly bedded intervals. Susceptibility and bulk density vary inversely with TOC. The abrupt drop in magnetic susceptibility has been dated at 3360 years B.P. [7].

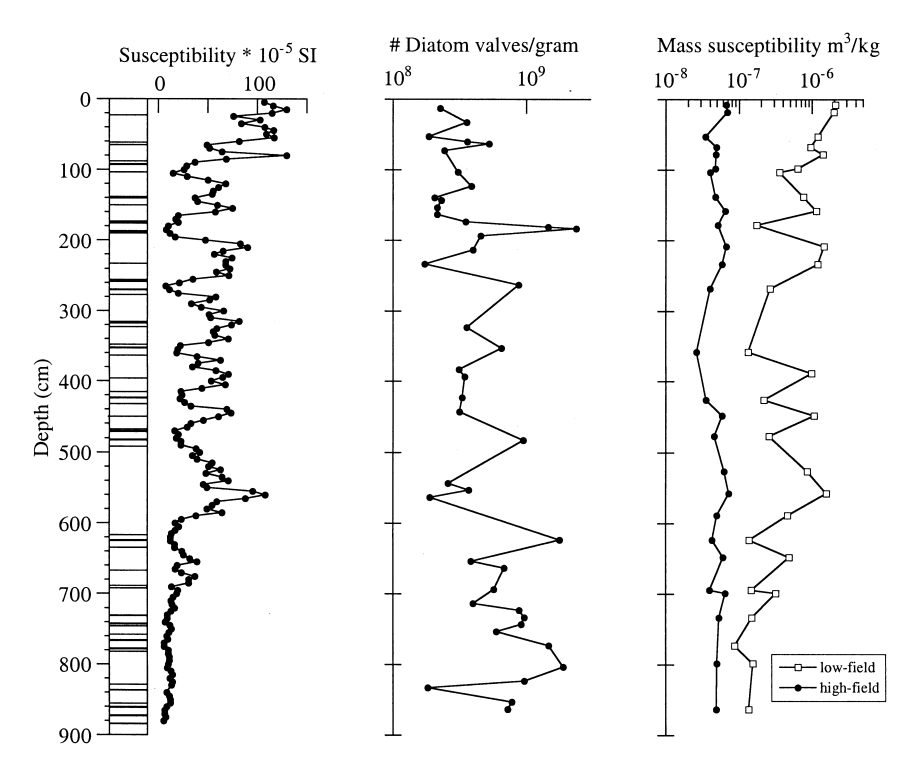


Fig. 3. Contribution of biogenic silica and paramagnetic minerals to bulk susceptibility of PD92-30. Bulk susceptibility varies inversely with the number of diatom valves per gram of sediment. In addition, intervals where bulk susceptibility is low have χ_{LF} only 2–3 times higher than χ_{HF} , indicating a lower concentration of ferrimagnetic phases in these intervals. Diatom data from [6].

green diatomaceous mud [5,6]. Values of magnetic susceptibility in the Palmer Deep are at least one order of magnitude lower than the sediments within nearby fjords, reflecting the relatively low abundance of ferrimagnetic minerals and a high abundance of biogenic silica [6]. Correlation with magnetic susceptibility records from nearby box cores and ODP Hole 178-1098C [11] indicates that at least 1.2 m of section is missing from the top of PD92-30.

Magnetic susceptibility shows a strong correspondence with sediment texture and physical properties (Fig. 2). Intervals of high magnetic susceptibility are massive and often burrowed, have a higher than average bulk density and lower than average total organic carbon (TOC) content. Intervals of low susceptibility are laminated and have a lower than average bulk density and higher than average TOC content [6]. Correlation coefficients for magnetic susceptibility with bulk den-

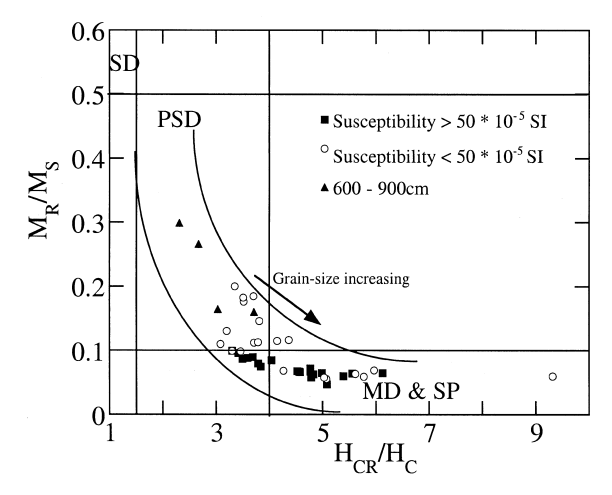


Fig. 4. Hysteresis parameters from PD92-30. Magnetic grain size increases from the upper left to the lower right of the diagram. Low-susceptibility intervals are generally finer-grained than high-susceptibility intervals. Below 600 cm, the magnetic grain size is PSD for both massive and laminated intervals. Redrawn after Leventer et al. [6].

sity, organic carbon content and diatom valves per gram of sediment are -0.616, -0.434 and -0.614, respectively. Ice-rafted debris (IRD) is uniformly distributed throughout the upper 600 cm of the core and decreases slightly below 600 cm [5,6]. The abrupt decrease in susceptibility at 600 cm in PD92-30 corresponds to slightly elevated values of TOC and higher abundance of diatom valves per gram of sediment, but there is no change in lithology at this horizon. Below 600 cm, the magnetic susceptibility remains low, although the alternation of massive and laminated intervals continues. This horizon has been dated at 3360 years B.P. and has been interpreted as a shift from a mid-Holocene climatic optimum to the onset of the Neoglacial period in the Antarctic Peninsula [7].

6. Magnetic granulometry

6.1. Concentration of magnetic material

Magnetic susceptibility varies inversely with the number of diatom valves per gram of sediment. Further, there is a consistent relationship between low-field (χ_{LF}) and high-field (χ_{HF}) susceptibility (Fig. 3). The latter parameter reflects the susceptibility of paramagnetic and diamagnetic phases. Massive intervals with high magnetic susceptibility are intervals where χ_{LF} is more than 10 times higher than χ_{HF} , indicating the dominance of ferrimagnetic phases. Intervals with low magnetic susceptibility are characterized by χ_{LF} of only 2-3 times higher than $\chi_{\rm HF}$, suggesting that in these intervals the diamagnetic and paramagnetic phases make a relatively higher contribution to the magnetic susceptibility. Therefore, the variability in the magnetic susceptibility signal reflects, in part, the variable dilution of terrigenous material by biogenic material. However, χ_{LF} undergoes larger amplitude changes than $\chi_{\rm HF}$. This suggests that the magnetic susceptibility record is not solely controlled by variable dilution. In addition, the high and low magnetic susceptibility intervals may have a different ferromagnetic and paramagnetic mineralogy.

6.2. Magnetic grain size

Hysteresis parameters show a bimodal distribution of grain sizes within the upper 600 cm of sediment in PD92-30 (Fig. 4). Intervals of high susceptibility ($>50\times10^{-5}$ SI) are characterized by hysteresis parameters that plot well within the multi-domain (MD) and superparamagnetic (SP) region of a 'Day Plot' [12], which corresponds to grain sizes larger than 10 µm (MD) and smaller than 0.3 µm (SP), respectively, for magnetite and titanomagnetite [13]. Low-temperature methods discussed below aid in distinguishing between MD and SP contributions to the magnetic mineral assemblage. Intervals of low susceptibility ($<50\times10^{-5}$ SI) are characterized by hysteresis parameters that straddle the boundary between the pseudo-single-domain (PSD) region and the MD region. Hysteresis parameters from samples below 600 cm fall in the middle of the PSD region (1-10 µm for magnetite and titanomagnetite), regardless of the massive or laminated texture of the sediment horizon.

6.3. Magnetic composition

Curie temperature measurements are shown in Fig. 5. High-susceptibility intervals (233 and 557 cm) are characterized by reversible thermomagnetic curves with Curie temperatures of 580– 590°C, indicative of pure magnetite. Low-susceptibility intervals (100, 188 and 358 cm) also have Curie temperatures of 580-590°C. However, these thermomagnetic curves are not perfectly reversible. Below 600 cm (693, 733 and 798 cm), the heating curves show significant decrease in $M_{\rm S}$ at 200–300°C and again at 500–580°C. M_S is higher for the cooling curve resulting from alteration of the sample during heating. Titanomagnetite (Fe_{3-x}Ti_xO₄, represented as TMx), titanohematite ($Fe_{2-x}Ti_xO_3$, represented as THx) and pyrrhotite all have Curie temperatures in the range 200-400°C, with the titanomagnetite and titanohematite Curie temperatures dependent on titanium content and oxidation degree. Iron sulfides often undergo alteration to a more stable phase (such as magnetite) during heating, causing

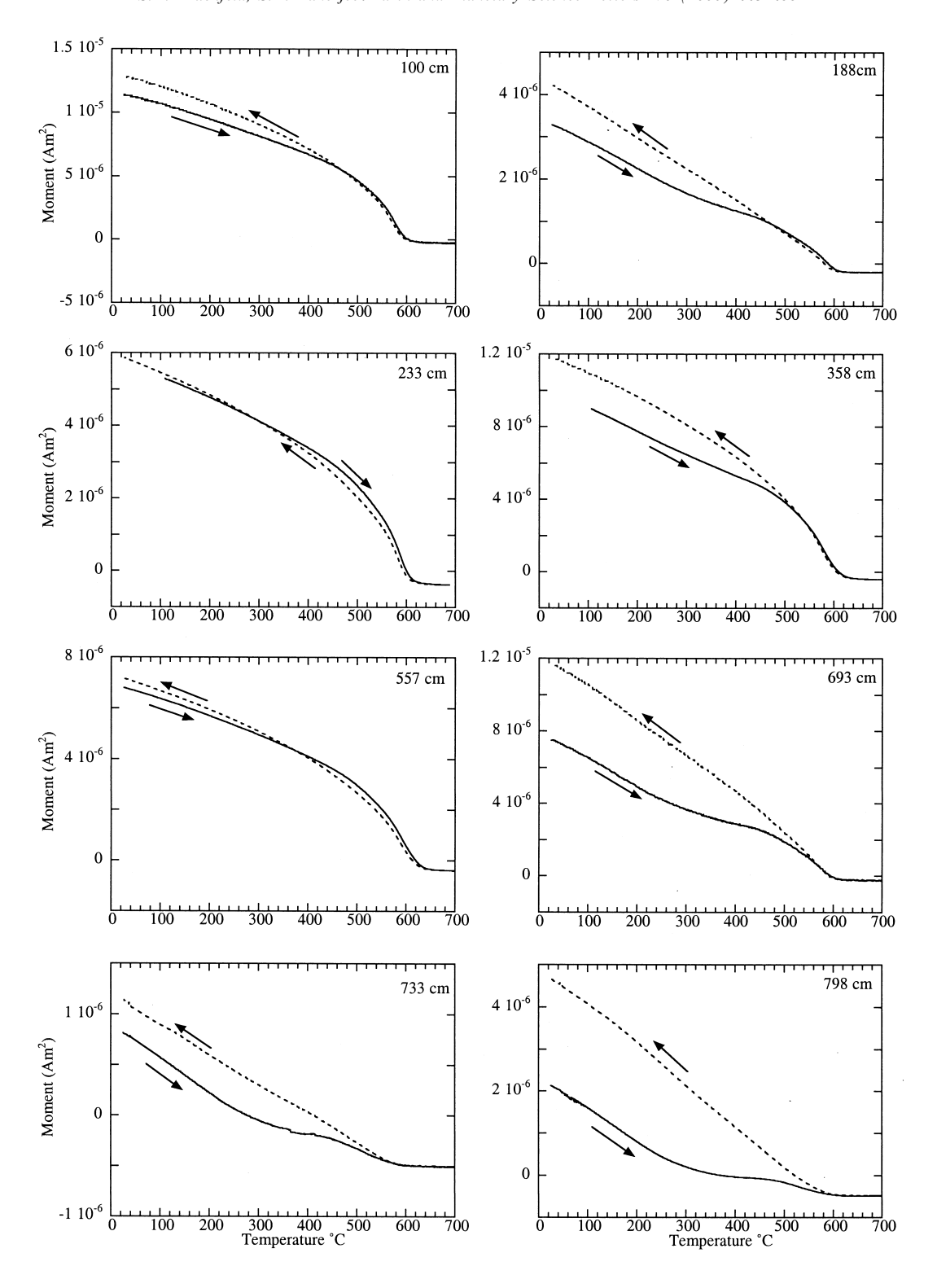


Fig. 5. Curie temperatures from PD92-30. High-susceptibility intervals (233 cm, 557 cm) have reversible heating (solid) and cooling (dashed) curves and magnetite Curie temperatures of 580–590°C. Low-susceptibility intervals in the upper 600 cm (100, 188 and 358 cm) have magnetite Curie temperatures, but the heating and cooling curves are not perfectly reversible. Samples from below 600 cm have irreversible curves that show unblocking over a low-temperature range (200–400°C) and over a high-temperature range (500–580°C).

an increase in saturation moment during heating, followed by a drop in the saturation moment at magnetite's Curie temperature. However, this was not observed in any of the Palmer Deep samples. The Curie temperatures observed here would correspond to TM28–TM60 or TH30–TH50. The two-phase behavior displayed by some of the Palmer Deep samples is more consistent with a titanium-rich phase (low Curie temperature) and a titanium-poor phase (high Curie temperature).

Low-temperature (20-300 K) measurements enable the examination of magnetic properties without thermochemical alteration. Several magnetic minerals undergo low-temperature crystallographic and thermomagnetic phase transitions that can be used as diagnostic indicators of that mineral's presence or absence, for example, pyrrhotite at 30-35 K, magnetite at 90-120 K and siderite at 35-40 K [14-16]. Samples from the upper 600 cm of PD92-30 (Fig. 6) show a sharp drop in the intensity of remanence, corresponding to the Verwey transition, at 106-110 K. The transition temperature is slightly lower than for pure magnetite, indicating some degree of cation substitution or non-stoichiometry. This transition is clear in samples from both high-susceptibility and low-susceptibility intervals. Samples from below 600 cm have mixed results. The sample from 693 cm has a slight drop in remanence at 110 K. Samples from 733 cm and 798 cm resemble lowtemperature curves of synthetic TM50-TM60 [17]. None of these samples displayed the pyrrhotite transition at 35 K.

Examination of magnetic susceptibility as a function of temperature and field frequency has been shown to be a useful tool in distinguishing compositional and grain size controls on low-temperature magnetic behavior [17–19]. Samples from the upper 600 cm show no frequency dependence of magnetic susceptibility at any temperature (Fig. 7), indicating minimal content of ultra-fine SP

grains. Samples from below 600 cm show frequency dependence at all temperatures from 20 to 300 K. For these samples χ_{FD} peaks at 6–14% over the interval 70–110 K, and drops to 2–5% at room temperature. Further, in these samples, susceptibility increases during warming to room temperature.

MD crystals of synthetic TM28-TM41 display strong frequency dependence over the tempera-

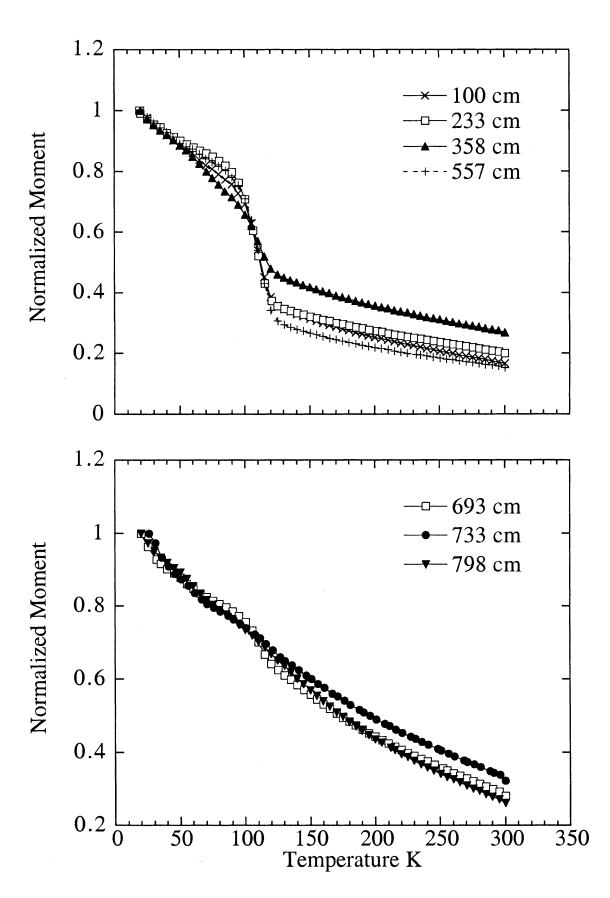


Fig. 6. Low-temperature remanence data from PD92-30. Samples were cooled to 20 K, given a remanence in a 2.5 T field, then warmed to room temperature. Samples from the upper 600 cm show Verwey transitions. Samples from below 600 cm have no clear low-temperature transitions.

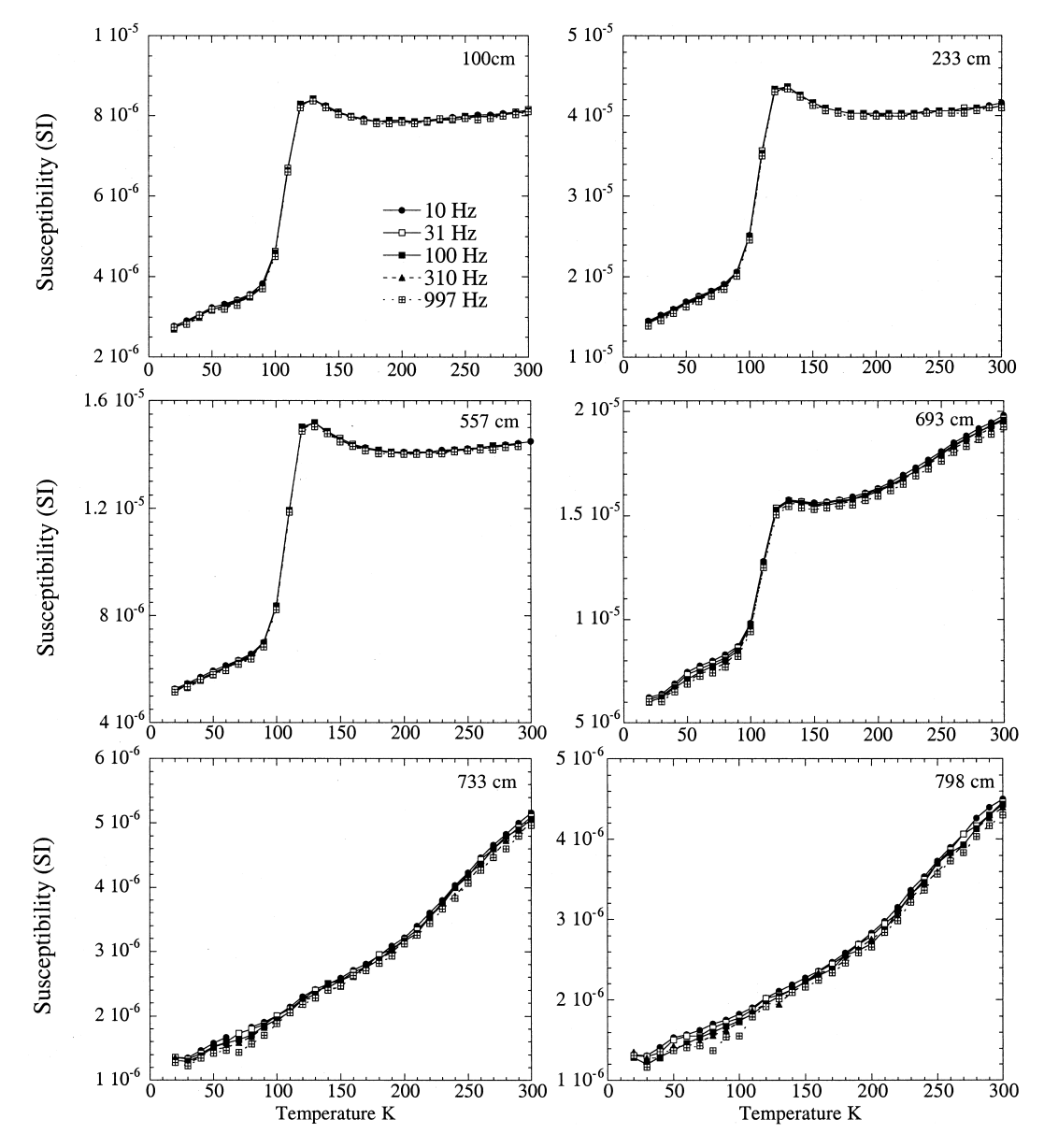
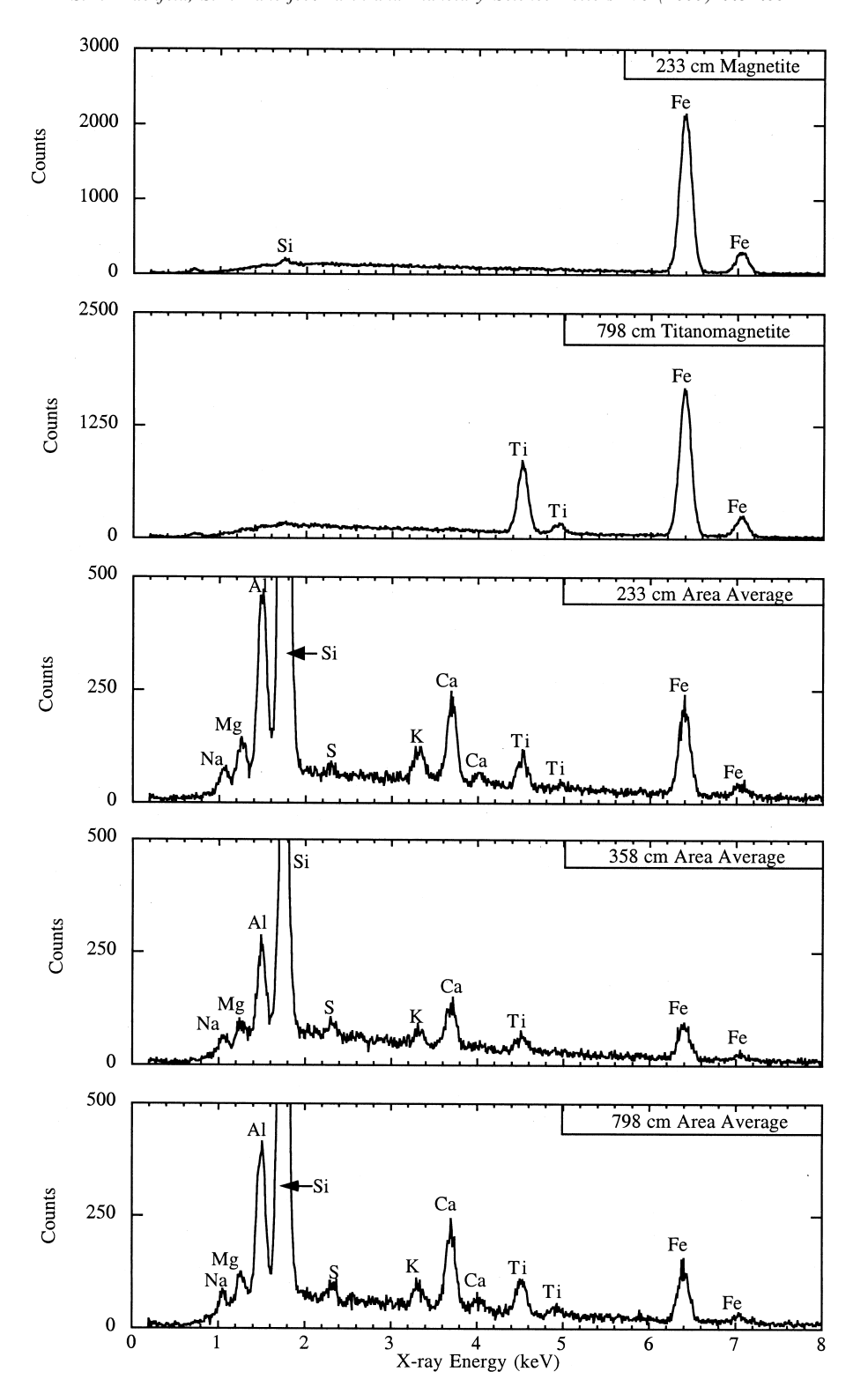


Fig. 7. Frequency dependence of susceptibility as a function of temperature for PD92-30. Samples from below 600 cm show χ_{FD} of 2-14% and increasing susceptibility during warming to room temperature, likely caused by the presence of titanomagnetite and ultra-fine SP particles.

Fig. 8. Energy-dispersive X-ray spectra (EDS). Individual grains from high-susceptibility intervals (e.g. 233 cm) have strong iron peaks. Individual grains from below 600 cm (e.g. 798 cm) have iron and titanium peaks. Individual grains from low-susceptibility intervals (not shown here) have spectra resembling the iron-only spectrum of 233 cm and the iron plus titanium spectrum of 798 cm. Area averages of high-susceptibility intervals have iron to titanium ratios of ~2:1. Low-susceptibility intervals (358 cm) and the interval below 600 cm have iron to titanium ratios of $\sim 1.3:1$. Sulfur is in the noise level of the area averages.



ture range of 50–150 K, but no frequency dependence above 150 K (M. Jackson, unpublished data). TM55 shows very slight frequency dependence over a narrow temperature range centered on 90 K (M. Jackson, unpublished data). TM28–TM60 show increasing susceptibility during warming up to room temperature due to a rapid decrease in magnetocrystalline anisotropy as a function of temperature [17]. However, SP magnetite may also cause an increase in susceptibility during warming up to room temperature if its grain volume is such that the blocking temperature is at or just above room temperature (e.g. [19]).

Low-temperature remanence and susceptibility data from samples below 600 cm likely result from a mixture of titanium-rich titanomagnetite and SP particles. Frequency dependence of susceptibility above 150 K is likely due to SP particles. Frequency dependence below 150 K could be due to either a compositional or grain size effect. The absence of remanence transitions, either the Verwey transition or a magnetic isotropic point, is consistent with a high-titanium titanomagnetite such as TM55–TM60 (e.g. [17]).

XRD and EDS spectra were obtained on magnetic extracts to further constrain the composition of the magnetic mineral assemblage. XRD spectra consistent with a spinel phase were identified in samples from above and below 600 cm. No peaks consistent with a hematite structure were seen. Therefore, the presence of titanohematite can be ruled out. There are no peaks consistent with any of the iron sulfides (e.g. pyrite, pyrrhotite or greigite). A cell parameter for the spinel phase was calculated from the average of the four highest intensity peaks. The sample from a high-susceptibility interval yielded a cell parameter of 8.387 Å, indicative of pure magnetite. We did not possess sufficient sediment from a low-susceptibility interval to concentrate the required amount of magnetic material interval for XRD analysis. The samples from below 600 cm yielded a cell parameter of 8.418 Å, consistent with TM30. However, all available data suggest a mixture of titaniumbearing phases in the sediment.

Representative EDS spectra are shown in Fig. 8. This is a standardless semiquantitative analysis

that measures relative elemental abundance and requires very little sample. Grains that appeared bright in backscatter electron images were selected for EDS analysis. A sample from 233 cm contains mostly magnetite, as indicated by EDS spectra containing only iron peaks. One pyrite framboid approximately 8 µm in diameter was observed in the extract from 233 cm. The EDS spectra of bright grains from 798 cm contain strong iron and titanium peaks, and are likely high-titanium titanomagnetite. One pyrite framboid approximately 3 µm in diameter was observed in the extract from 798 cm. Individual grains from 358 cm, a low-susceptibility interval, yielded EDS spectra similar to both the iron-only spectrum of 233 cm and the iron plus titanium spectra of 798 cm.

EDS spectra were also obtained from large $4~\rm mm^2$ areas referred to as 'area averages', which were scanned by the electron beam at the lowest magnification $(40\times)$ in order to obtain a rough bulk chemistry. All intervals have area averages containing iron, titanium, calcium, potassium, magnesium and sodium (Fig. 8). However, there are differences in the amplitudes of the iron and titanium peaks. Generally, the samples from high-susceptibility intervals have iron peaks that are at least twice as high as the titanium peaks. In samples from low-susceptibility intervals (358 cm) and below 600 cm (693 cm), the iron peak is 1.2–1.4 times the amplitude of the titanium peak.

7. Discussion

On the basis of preliminary results presented in [6] and [20], it was suggested that the variation in magnetic susceptibility could be due to a primary depositional process, iron-sulfur diagenesis, or a combination of the two. On the basis of the rock-magnetic investigations presented here, diagenesis can now be considered a minor control on the susceptibility profile. The olive green facies and the presence of pyrite framboids indicate that ferrous iron has been mobile in the sediments. However, these chemical changes have not obscured the primary depositional signal.

Reductive dissolution of magnetite typically results in the coarsening of the overall magnetic

mineral assemblage as finer grains are preferentially dissolved (e.g. [21]). Magnetite dissolution has been observed to coincide with high TOC content in marine sediments (e.g. [22]). The Palmer Deep sediments show coarse MD grains in high-susceptibility, low TOC intervals, smaller PSD grains in the low-susceptibility, high TOC intervals, and fine PSD and SP grains in the very low-susceptibility, very high TOC interval below 600 cm. It is possible that the high-susceptibility intervals have been coarsened due to dissolution of finer grains. However, in this scenario, we would expect the SP grains to have dissolved as well.

None of the rock-magnetic data showed evidence of magnetic iron sulfides in these sediments (e.g. pyrrhotite and greigite). Pyrite framboids were observed in both the high- and low-susceptibility intervals. However, sulfur was within the noise level of the EDS spectra, suggesting that sulfides are a relatively minor component of the sediment assemblage.

Interstitial water data collected onboard the R.V. Joides Resolution during ODP Leg 178 indicate that organic matter degradation and sulfate reduction occur at 20–30 m below seafloor [11], substantially deeper than the drop in magnetic susceptibility. Unfortunately, the iron data, the element of greatest relevance to this problem, was consistently below the detection limit of the instrument onboard the R.V. Joides Resolution. No chemical boundaries were observed to coincide with the susceptibility drop. We therefore consider the magnetic susceptibility record of the Palmer Deep to be a paleoenvironmental signal with minor diagenetic overprinting.

The late Holocene sediments of core PD92-30 display three distinct magnetic mineral assemblages. High-susceptibility intervals in the upper 600 cm contain high concentrations of MD magnetite. Leventer et al. [6] interpreted these intervals as times of increased windiness and/or storm frequency. Under these conditions, the water column is very well mixed and diatoms have a relatively short residence time in the photic zone, which limits productivity. Terrigenous sedimentation dominates over biogenic sedimentation, causing

a relative high in magnetic susceptibility. The MD magnetite grains are likely derived from the plutonic rocks of Graham Land and carried 20 km offshore to the Palmer Deep by ice-rafting.

Low-susceptibility intervals in the upper 600 cm contain lower concentrations of magnetic material and considerably more biogenic material. The diatom assemblage within these intervals is dominated by *Chaetoceros* resting spores and contains diatom species seeded to the water column by melting sea ice [6]. These intervals were interpreted as times of a meltwater-stratified water column that is conducive to diatom blooms [1,6]. These are times of higher particle fluxes to the seafloor and biogenic sedimentation dominates over terrigenous sedimentation. The lower susceptibility values are also a function of magnetic mineralogy. The low-susceptibility intervals are characterized by finer-grained PSD magnetite and titanomagnetite that have inherently lower susceptibility than MD pure magnetite. This implies a change in the energy of the sediment transport mechanism, possibly a reduction in IRD or a change in sediment provenance.

The interval below 600 cm is characterized by a very low abundance of magnetic material. The magnetic mineral assemblage consists of PSD titanium-rich titanomagnetite and SP particles. This interval has overall higher levels of TOC and biogenic silica [5–7], which suggests higher levels of productivity. The magnetic data are consistent with these more traditional proxies. The production of SP magnetite has been observed in laboratory cultures of dissimilatory Fe (III) reducing bacteria (e.g. [23]), and it has been proposed that SP magnetite is an indicator of enhanced productivity in marine sediments (e.g. [24]).

The more striking observation is the complete absence of MD magnetite below 600 cm. MD magnetite was the sole magnetic phase observed in a suite of plutonic rocks from Northern Graham Land (Brachfeld and Grunow, in preparation). Its absence in the sediments suggests a cessation in locally derived IRD, resulting in a magnetic mineral assemblage dominated by titanomagnetite derived from further afield.

8. Conclusions

A cyclic magnetic susceptibility signal observed in glacial-marine sediment cores from the western Antarctic Peninsula was the primary motivation for the detailed rock-magnetic study of core PD92-30. This record does not appear to have been significantly affected by post-depositional diagenetic alteration of the magnetic minerals. Three distinct magnetic mineral assemblages were observed in PD92-30. In the upper 600 cm, intervals of high magnetic susceptibility are dominated by MD magnetite, likely input to the Palmer Deep via ice-rafting. Intervals of low magnetic susceptibility contain higher than average biogenic silica and TOC content. Low values of magnetic susceptibility result from the dilution of the terrigenous sediments with biogenic silica and shifts in the magnetic grain size and mineralogy to PSD magnetite and titanomagnetite. The interval below 600 cm is characterized by very low abundance of magnetic material. The magnetic mineral assemblage consists of titanium-rich titanomagnetite plus ultra-fine SP particles. This assemblage is consistent with increased productivity and reduced IRD. This horizon has been dated at 3360 years B.P., and may represent changing provenance and sediment transport patterns during the mid-Holocene climatic optimum.

Acknowledgements

We thank Amy Leventer, Eugene Domack, Pat Manley and Mike Jackson for helpful discussions and Emily Youcha for laboratory assistance. David Williamson, Leah Joseph and Carl Richter provided thoughtful reviews that improved this manuscript. This work was supported by the National Science Foundation Office of Polar Programs Grant OPP-9615695. This is IRM contribution #9907. The IRM is supported by grants from the Earth Sciences Division of the National Science Foundation and the W.M. Keck Foundation./RVI

References

- R. Smith, E.W. Domack, S. Emslie, W. Fraser, D. Ainley, K. Baker, J. Kennett, A. Leventer, E. Mosely-Thompson, S. Stammerjohn, M. Vernet, Marine ecosystem sensitivity to climate change, Bioscience 49 (1999) 393–404.
- [2] E.W. Domack, S.E. Ishman, Oceanographic and physiographic controls on modern sedimentation within Antarctic fjords, Geol. Soc. Am. Bull. 105 (1993) 1175–1189.
- [3] A. Leventer, Sediment trap diatom assemblages from the northern Antarctic Peninsula region, Deep Sea Res. 38 (1991) 1127–1143.
- [4] E.W. Domack, S.E. Ishman, Magnetic susceptibility of Antarctic glacial marine sediments, Antarct. J. U.S. 27 (1992) 64–65.
- [5] M.E. Kirby, E.W. Domack, C.E. McClennen, Magnetic stratigraphy and sedimentology of Holocene glacial marine deposits in the Palmer Deep, Bellingshausen Sea, Antarctica: implications for climate change?, Mar. Geol. 152 (1998) 247–259.
- [6] A. Leventer, E.W. Domack, S.E. Ishman, S. Brachfeld, C.E. McClennen, P. Manley, Productivity cycles of 200– 300 years in the Antarctic Peninsula region: understanding linkages between the Sun, atmosphere, sea ice and biota, Geol. Soc. Am. Bull. 108 (1996) 1626–1644.
- [7] E.W. Domack, A. Leventer, R. Dunbar, F. Taylor and S. Brachfeld, The Holocene, ODP Leg 178 Shipboard Scientific Party, Holocene climate variability in the Antarctic Peninsula in prep.
- [8] E.W. Domack, P.A. Mayewski, Bi-polar ocean linkages evidence from late-Holocene Antarctic marine and Greenland ice-core records, Holocene 9 (1999) 247–251.
- [9] M. Rebessco, A. Camerlenghi, L. DeSantis, E.W. Domack, M.E. Kirby, Seismic stratigraphy of Palmer Deep: a fault bounded late Quaternary sediment trap on the inner continental shelf, Antarctic Peninsula Pacific margin, Mar. Geol. 151 (1998) 89–110.
- [10] S. Brachfeld, Separating geomagnetic paleointensity and paleoclimate signals in sediments: examples from North America and Antarctica, Ph.D. dissertation, Univ. Minnesota, Minneapolis, MN, 1999.
- [11] P.F. Barker, A. Camerlenghi, G. Acton et al., Proc. Ocean Drilling Program, Initial Reports, 178, 1998.
- [12] R. Day, M.D. Fuller, V.A. Schmidt, Hysteresis properties of titanomagnetites: Grain size and composition dependence, Phys. Earth Planet. Int. 13 (1977) 260–266.
- [13] D.J. Dunlop, Hysteresis properties of magnetite and their dependence of particle size: a test of pseudo-single-domain remanence models, J. Geophys. Res. B 91 (1986) 9569–9584.
- [14] P. Rochette, G. Fillion, J.-L. Mattéi, M.J. Dekkers, Magnetic transition at 30–34 Kelvin in pyrrhotite: insight into a widespread occurrence of this mineral in rocks, Earth Planet. Sci. Lett. 98 (1990) 319–328.

- [15] Ö. Özdemir, D.J. Dunlop, B.M. Moskowitz, The effect of oxidation on the Verwey transition in magnetite, Geophys. Res. Lett. 20 (1993) 1671–1674.
- [16] B.A. Housen, S.K. Banerjee, B.M. Moskowitz, Low-temperature magnetic properties of siderite in marine sediments, Geophys. Res. Lett. 23 (1996) 2843–2846.
- [17] B.M. Moskowitz, M. Jackson, C. Kissel, Low-temperature magnetic behavior of titanomagnetites, Earth Planet. Sci. Lett. 157 (1998) 141–149.
- [18] M.J. Jackson, B.M. Moskowitz, J. Rosenbaum, C. Kissel, Field-dependence of AC susceptibility in titanomagnetites, Earth Planet. Sci. Lett. 157 (1998) 129–139.
- [19] H.-U. Worm and M. Jackson, The superparamagnetism of Yucca Mountain tuff, J. Geophys. Res. B, 1999 (in press).
- [20] S.A. Brachfeld, A. Leventer, E.W. Domack, Holocene paleoclimate records from Antarctic glacial–marine sediments: rock magnetic and biologic indicators of paleopro-

- ductivity, EOS Trans. Am. Geophys. Union 76 (1995) F161
- [21] R. Karlin, Magnetite diagenesis in marine sediments from the Oregon continental margin, J. Geophys. Res. B 95 (1990) 4405–4419.
- [22] J.A. Tarduno, Temporal trends of magnetic dissolution in the pelagic real: gauging paleoproductivity?, Earth Planet. Sci. Lett. 123 (1994) 39–48.
- [23] D.R. Lovely, Magnetite formation during microbial dissimilatory iron reduction, in: R.B. Frankel and R.P. Blakemore (Eds.), Iron Biominerals, Plenum Press, 1991, pp. 151–166.
- [24] J.A. Tarduno, Superparamagnetism and reduction diagenesis in pelagic sediments: enhancement or depletion?, Geophys. Res. Lett. 22 (1995) 1337–1340.
- [25] M. Rebessco, A. Camerlenghi, C. Zanolla, Bathymetry and Morphogenesis of the Continental Margin west of the Antarctic Peninsula, Terra Antarct. 5 (1998) 715–725.